Volume 1 No. 2, August 2011
International Journal of Science and Technology

http://www.ejournalofsciences.org

Nucleation, growth and characterization of Bis(thiourea) cadmium formate NLO single crystals

[1]S.M. Ravi Kumar, [2]S.Selvakumar, [3]S.Kiruba, [4]M.Tholkappian, [5]P.Sagayaraj
[1,4]PG & Research Department of Physics, Govt. Arts College, Thiruvannamalai-606 603
[2]Department of Physics, L.N. Government College, Ponneri- 601 204
[3]Department of Physics, Sacred Heart College, Thriupattur-635 601
[5]Department of Physics, Loyola College, Chennai 600 034

ABSTRACT

Growth of bis (thiourea) cadmium formate single crystals from aqueous solution by slow evaporation technique has been reported. To optimize the growth conditions, nucleation parameters such as metastable zone width and induction period values are determined. The grown crystals are characterized by powder XRD technique. Thermal studies by TGA and DTA techniques confirm the decomposition of the sample around 190 ºC. The *dc* conductivity study shows that the conductivity of BTCF increases with temperature. The laser damage threshold of the BTCF is found to be higher than KDP. The UV-Vis-NIR spectral analysis confirms the cut off wavelength of the sample around 290 nm with a wide transmission window (290 nm-2000 nm)

Keywords: *Organometallic, nucleation parameters, thermal, laser damage threshold, dc conductivity*

1. INTRODUCTION

Nonlinear optical (NLO) organometallic complexes are given much attention because of their ability to combine the flexibility of organic materials with the thermal stability and mechanical strength of inorganic materials [1]. Thiourea is one of the few simple organic compounds with high crystallographic symmetry. It crystallizes in the rhombic bipyramidal division of rhombic system and acts as a good ligand [2]. The centrosymmetric thiourea molecule, when combined with inorganic salts yields noncentrosymmetric complexes, which possess good nonlinear optical properties [3]. Thiourea possess large dipole moment and it forms number of NLO active metal coordination compounds like Bis(thiourea) cadmium chloride (BTCC) [4], Bis(thiourea) zinc chloride [5], Bis(thiourea) cadmium acetate [6], Zinc tri(thiourea) sulfate (ZTS) [7], Dichloro detrakis thiourea nickel (NTC) [8], etc,. Among these, organometallic NLO crystal of BTCF is a recently developed material with promising properties of laser application, and preliminary studies such as single crystal XRD, mechanical and optical transmission has been already reported by our group [9].

In order to improve the growth mechanism, the metastable zone width and induction period are determined experimentally along with the nucleation parameters such as interfacial energy, radius of critical nucleus and critical free energy barrier. Bulk size crystals of BTCF are grown by slow evaporation method. Since thiourea has a tendency to form multiple phases with metals, a well documented powder pattern can be useful in assessing the homogeneity of the material [7]. Hence, the grown crystal is characterized by powder XRD. BTCF crystals are also subjected to optical absorption, laser damage threshold, thermal and *dc* conductivity studies.

2. EXPERIMENTAL

2.1 Metastable zone width and induction period

The metastable zone width of BTCF in aqueous solution was measured by polythermal method [10]. About 100 ml of the saturated solution of BTCF prepared in accordance with the solubility data was taken in a round bottom nucleation flask. The studies were carried out in a constant temperature bath with cryostat facility. The bath is capable of controlling the temperature with an accuracy of ± 0.01 °C. The solution was preheated to 5 °C above the saturation temperature and left at the superheated temperature for 1 hour before cooling. Homogenization of the solution was ensured by stirring the solution with a motorized stirrer throughout the experiment. The temperature of the bath was reduced at the rate of 5 °C per hour while stirring the solution continued. The temperature at which the first speck of the nucleus is visible will correspond to the width of the metastable zone. The experiment was repeated for solutions saturated at different temperatures (30, 35, 40 and 45 °C).

The metastable zone width of BTCF for different temperatures is shown in figure 1. It is seen from the plot that the zone width decreases with increase in temperature. Induction period was also measured by isothermal method [11]. The saturated solution was cooled to the desired temperature and by maintaining at that temperature the time taken for the formation of the first speck of the nucleus was noted. Induction period of BTCF was recorded for different supersaturation ratios of 1.1, 1.2, 1.3 and 1.4. Figure 2 shows the induction period as a function of supersaturation for BTCF. The study of induction period at different supersaturation levels gives an idea of the optimized induction period to have controlled nucleation rate to facilitate the growth of bulk size single

crystals. For BTCF, the induction period is found to decreases with increase in supersaturation.

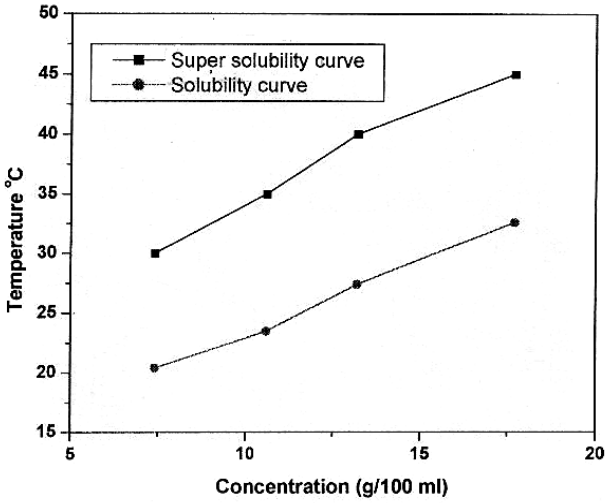

Figure 1 Metastable zone width of BTCF as a function of temperature

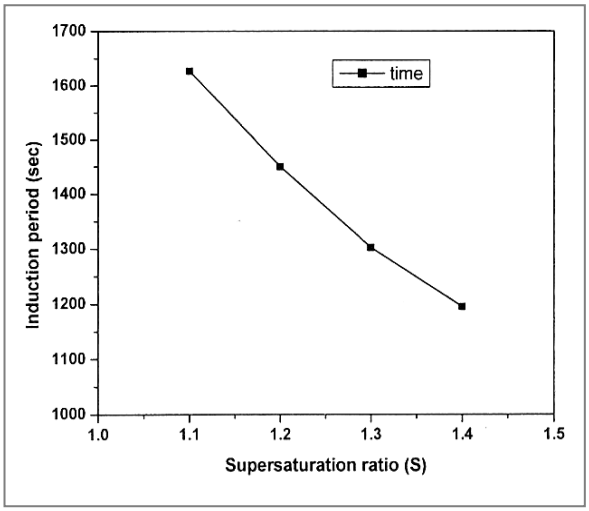

Figure 2: Induction period vs supersaturation of BTCF

2.2 Nucleation parameters

In the present work, the nucleation parameters of BTCF have also been evaluated. The change in the Gibbs free energy (ΔG) between the crystalline phase and the surrounding mother solution results in a driving force, which stimulates crystallization. According to classical nucleation theory the free energy required to form a spherical nucleus is given by $\Delta G = (4/3)\ \pi r^3\ \Delta G_V + 4\pi r^3 \gamma$, where, ΔG_V is the energy change per unit volume, r is the radius of the nucleus and γ is the interfacial energy. The nucleation parameters such as, ΔG_V, γ and critical nucleus (r*) are calculated by using the well known formulate [12 & 13] and the same are presented in Table 1.

Table 1 Nucleation parameters of BTCF

Super-saturation Ratio 'S'	Induction period 'τ' sec	Energy change per unit volume ΔV ($x10^6$ erg/cm^3)	Free energy formation GV* (($x10^{-21}$ Joule)	Critical radius 'r*' ($x10^{-10}$ m)
1.1	1627	-1.5342	6.340	12.54
1.2	1450	-2.935	1.0912	5.621
1.3	1302	-4.223	0.320	3.308
1.4	1195	-5.416	0.112	2.141

It is observed from the table that the nucleation rate increases with supersaturation ratio, which means the formation of higher number of nuclei with increased supersaturation. The free energy barriers for formation of critical nucleus size decreased with increasing supersaturation ratio. The nuclei will become stable and grow faster if the energy barrier is reduced at high supersaturation ratios. The free energy barriers for formation of critical size nucleus at supersaturation of 1.1and 1.4 are 6.34 x $l0^{-21}$ and 0.112 x 10^{-21}J respectively. The interfacial tension of BTCF was estimated as 2.57 mJ/m^2 from the slope of *ln* τ and (*ln* S)$^{-2}$ curve [14] (Figure 3).

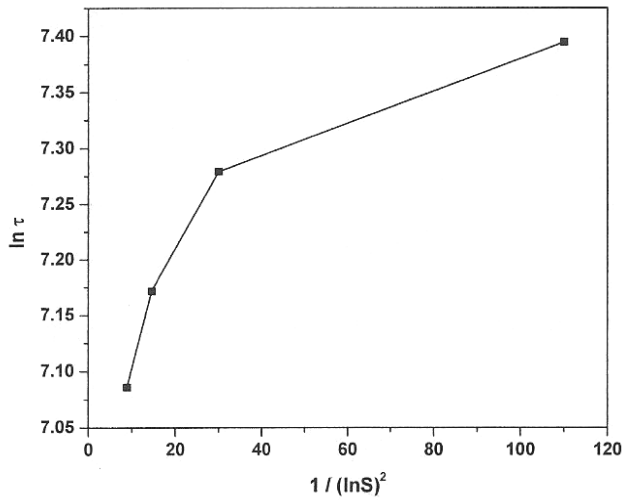

Figure 3 Relation between *ln* τ and *(lnS)*$^{-2}$ for BTCF

2.3 Crystal Growth

The saturated solution of Bis (thiourea) cadmium formate was prepared in accordance with the solubility data by dissolving cadmium oxide, formic acid and thiourea in the stiochiometric ratio 1:2:2 in Millipore water. The solution was constantly stirred for one day to avoid co-precipitation of multiple phases. The stirred solution was filtered and then allowed to evaporate at room temperature (303 K). In a period of 5-10 days, seed crystals of BTCF were formed due to spontaneous nucleation. Optically good grade tiny crystals with perfect

shapes were selected as seeds to grow bulk size crystals. Crystal having dimension upto 25 x 10 x 2 mm^3 was harvested in a period of 50-60 days (Figure 4).

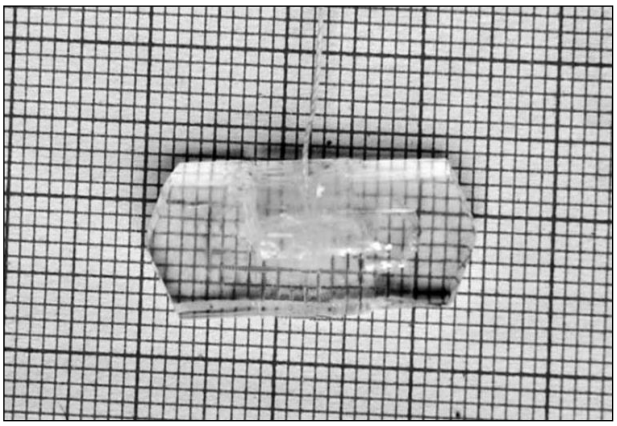

Figure 4 Photograph of as grown crystal of BTCF

3. CRYSTAL CHARACTERIZATION

3.1 Powder X-ray Diffraction Analysis

X-ray powder diffraction (XRPD) pattern of BTCF was recorded on a Rich Seifert diffractometer with Cuk_α (λ = 1.5418 Å) radiation. The powder sample was scanned over the range 10 - 70° at a scan rate of 1°/ min. The XRPD pattern of the crystal is shown in Figure 5. The observed 'd' values for different 2θ with (h k l) indices of the corresponding reflecting planes for the crystal are given in Table 2. The XRPD peaks are indexed and unit cell parameters are calculated with the help of the TERROR program. The unit cell parameters are a = 8.012 Å, b = 17.755 Å, c = 3.890 Å, V = 553.365 $Å^3$, which are in good agreement with the results reported by single crystal XRD [9].

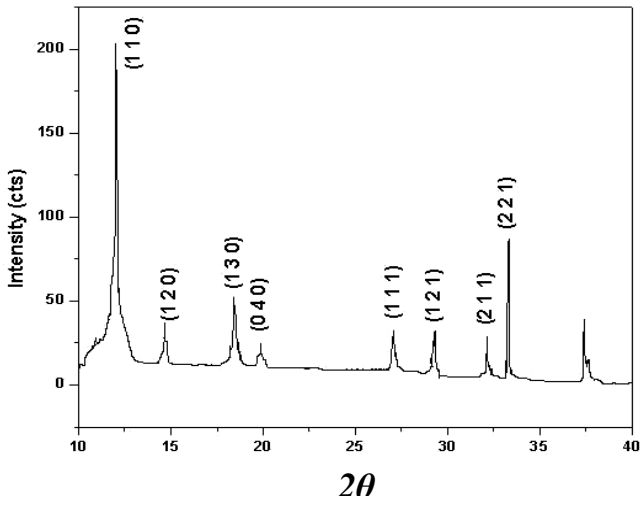

Figure 5 Indexed powder XRD pattern of BTCF

Table 2 Powder X-ray diffraction data for BTCF

2θ	$d_{calculated}$	$d_{observed}$	(h k l)
12.131	7.295	7.301	110
14.901	5.491	6.021	120
18.637	4.755	4.942	130
19.994	4.433	4.489	040
25.851	3.446	3.495	111
27.301	3.266	3.281	121
32.236	2.772	2.801	160
32.416	2.753	2.762	211
33.589	2.667	2.670	221

3.2 DC Conductivity Studies

A polished sample of BTCF with known dimension was subjected to dc electrical conductivity study. The resistance of the sample along (1 0 0) plane was measured at a fixed frequency (10 KHz) using million megohmmeter with the conventional two probe method. The resistance was measured at different temperatures (40 to 100 °C). The dc electrical conductivity (σ_{dc}) of BTCF was calculated by the relation, σ_{dc} = d/RA, where, R is the measured resistance, d is the thickness of the sample and A is the area of the sample. The σ_{dc} values were fitted in to the equation $\sigma_{dc} = \sigma_o \exp(-E_{dc}/KT)$ and the activation energy (E_{dc}) was calculated.

The temperature dependence of the dc conductivity for BTCF crystal is shown in figure 6. The conductivity of the sample almost shows a linear relationship with temperature. The influence of the temperature on conductivity can be explained by considering the mobility of charge carrier responsible for hopping. As temperature increases the mobility of hopping ions also increases which in turn tend to increase the conductivity. The electrons which are involved in hopping are responsible for electronic polarization in this crystal [15]. The activation energy of BTCF is found to be 0.37 eV from figure 6.

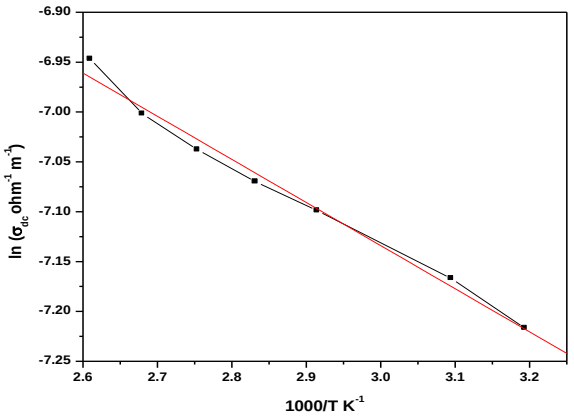

Figure 6 Temperature dependent conductivity of BTCF

3.3 Thermal Studies

Thermogravimetric analysis (TGA) and differential thermal analysis (DTA) of the BTCF crystal were carried out using a NETZSCH STA 409C thermal analyzer. The sample (34.68 mg) was heated in a aluminum crucible between 23 and 1300 ºC at a heating rate of 10 K/min in nitrogen atmosphere.

The TGA/DTG traces of BTCF are illustrated in figure 7. The decomposition starts around 190 ºC and produces a sharp weight loss of 29 % which is followed by another weight loss of about 21 %. Since the decomposition does not leave any residue, Cd is expected to escape as a volatile. This will be possible, if it produces a compound with the organic residue of volatile nature. Since, there is no weight loss below 190 ºC, the crystal is devoid of physically adsorbed water or water of crystallization.

The DTA trace of BTCF is illustrated in figure 8. There is a sharp endotherm with a maximum at 191.7 ºC. This endotherm coincides with the weight loss in TGA trace (figure 7) and thus confirming that the crystal decomposes without melting. The absence of any endo or exotherm below 190 ºC also supports this discussion.

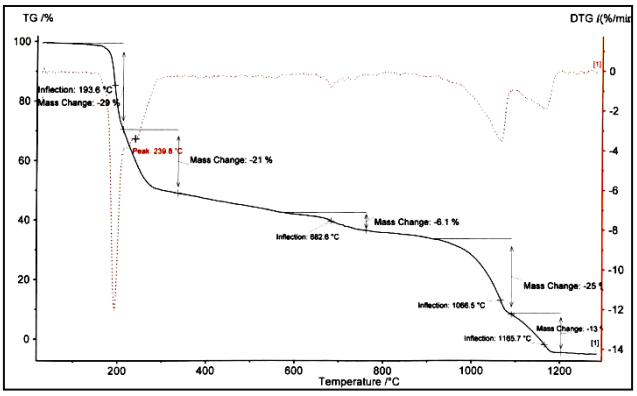

Figure 7 TGA trace of BTCF

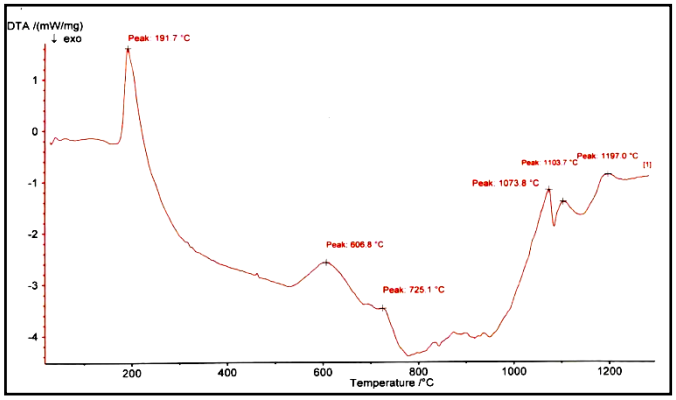

Figure 8 DTA trace of BTCF

3.4 Laser damage threshold measurement

Multiple mode laser damage measurement is made on the (1 0 0) orientation of the BTCF crystal. The experimental setup for laser damage threshold is illustrated with detail [16]. BTCF crystal with a thickness of 2 mm was mounted on a sample holder. BTCF was irradiated by multiple pulse mode Nd:YAG laser with 1064 nm wavelength and 8 ns pulse duration. The laser was operated at a repetition rate of 10 Hz. A 8 mm diameter incident beam was focused onto the sample by convex lens of focal length 40 cm. The radius of the focused spot of the Nd:YAG laser beam was estimated to be 20.4 μm. The damage threshold of BTCF for the multiple shot was found to be 7.623 GW/cm^2. The damage threshold of BTCF is compared with other NLO crystals (Table 3) [16, 17]. From the table it is observed that BTCF can be used for high power frequency conversion application.

Table 3 Comparison of Laser damage threshold of BTCF with other popular NLO crystals

Crystal Name	Laser damage threshold (GW/cm^2)
BTCF	7.623
BTCC	6.0
ZTS	7.8
KDP	0.20
Urea	1.50

3.5 Linear optical property

The optical absorbance of BTCF crystal was recorded using VARIAN CARY 5E model spectrophotometer in the wavelength range 200 – 2000 nm. The optical absorption spectrum of BTCF is shown in figure 9. The cut-off wavelength as observed from the absorption spectrum is 290 nm. The crystal has very low absorption in the entire visible and NIR regions. The large transmittance window in the visible and NIR regions enables very good optical transmission of the second harmonic frequencies of Nd:YAG laser.

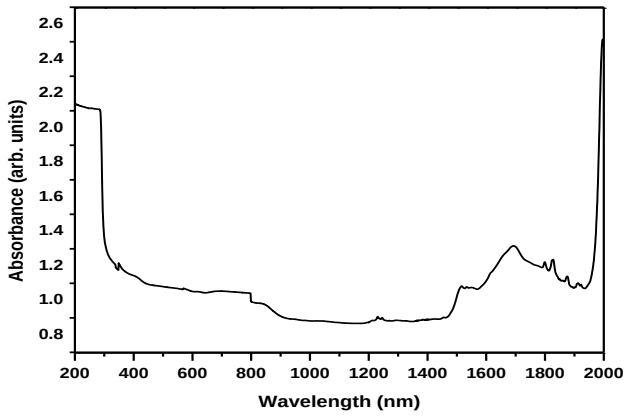

Figure 9 Optical absorption spectrum of BTCF

4. CONCLUSION

Organometallic NLO crystals of BTCF were successfully grown by slow evaporation method. The nucleation kinetics of BTCF was studied at different supersaturation ratios. The induction time for nucleation of BTCF is found to decrease with increase in supersaturation ratio. The grown crystal was confirmed by powder XRD. The temperature dependence *dc* conductivity study of BTCF shows that the conductivity increases with temperature. TGA/DTA analysis implies that BTCF is stable upto 190 ºC before its melts. Multiple-shot damage of BTCF was observed at an energy density of 7.623 GW/cm^2. Significant wider optical transparency and lower cut-off wavelength down to 290 nm makes it a promising material for NLO applications.

REFERENCES

[1] P.R. Newman, L.F. Warren, P. Cunningham, T.Y. Chang, D.E. Copper, G.L. Burdge, P. Polak dingels and C.K. Lowe-Ma, Materials Research Society Symposium Proceedings, 173(1990) 557.

[2] S.B. Hendricks, J. Am. Chem. Soc. 50(1928)2455.

[3] S. Anie Roshan, Cyriac Joseph and M.A. Ittyachen, Materials Letters, 49 (2001) 299.

[4] S.Selvakumar, J.Packiam Julius, S.A. Rajasekar, A.Ramanand, P.Sagayaraj, Mater. Chem. And Phys. 93 (2005)356.

[5] S.Selvakumar, K.Rajarajan, S.M. Ravi kumar, I. Vetha Potheher, D. Premanand, P.Sagayaraj, Cryst. Res. Tech. 41 (2006)766.

[6] N.P.Rajesh, V.Kannan, M.Ashok, K.Shivaji, P.Santhana Raghavan, P.Ramasamy, J.Crystal Growth, 262 (2004) 561.

[7] V.Venkataraman, G.Dhanaraj, V.K.Wadhawan, J.N. Sherwood and H.L. Bhat, J.Cryst. Growth, 154 (1995) 92.

[8] K.Ambujam, P.C. Thomas, S.Aruna, D.Prem Anand, P.Sagayaraj, Cryst. Res. Tech. 41 (2006) 1082.

[9] S.Selvakumar, S.M.Ravi kumar, K.Rajarajan, A.Joseph Arul Pragasam, S.A.Rajasekar, K.Thaimzharasan, P.Sagayaraj, Crystal Growth and Design, 6 (2006)2607.

[10] J.Nyvlt, J.Crystal Growth, 3 (1968) 377.

[11] N.P.Zaiteseva, L.N,Rakovich, S.V.Bagatyareva, J.Crystal Growth, 148 (1995) 276.

[12] H.El.Shall, Jin-hwan Jen, E.A. Abdel-Aal, S.Khan, L.Gower and Y.Rabinovich, Cryst. Res. Tech. 39 (2004) 214.

[13] T.Kanagasekaran, M.Gunasekaran, P.Srinivasan, D.Jayaraman, R.Gopalakrishnan and P. Ramasamy, Cryst. Res.Tech. 40 (2005) 1128.

[14] R.Sankar, C.M.Raghavan and R.Jayavel, Cryst. Res. Tech. 41 (2006) 919.

[15] S.Sindhu, M.R.Anatharaman, Bindhu P. Thampi, K.A.Malini and Philip Kurian, Bull. Mater. Sci., 25 (2002) 599.

[16] N.Vijayan, G.Bhagavannarayana,T.Kanagasekaran, R.Ramesh Babu, R.Goplakrishnan and P. Ramasamy, Cryst. Res. Tech. 41 (2006) 784.

[17] V.Venkataramanan, C.K.Subramanian and H.L.Bhat, J.Appl. Phys. 77 (1995) 6049.